

# Engineering Yeast Peroxisomes for $\alpha$ -Bisabolene Production from Sole Methanol with the Aid of Proteomic Analysis

Published as part of JACS Au virtual special issue "Biocatalysis in Asia and Pacific."

Linhui Gao,<sup>1</sup> Rui Hou,<sup>1</sup> Peng Cai, Lun Yao, Xiaoyan Wu, Yunxia Li, Lihua Zhang,\* and Yongjin J. Zhou\*



Cite This: JACS Au 2024, 4, 2474–2483



Read Online

ACCESS |

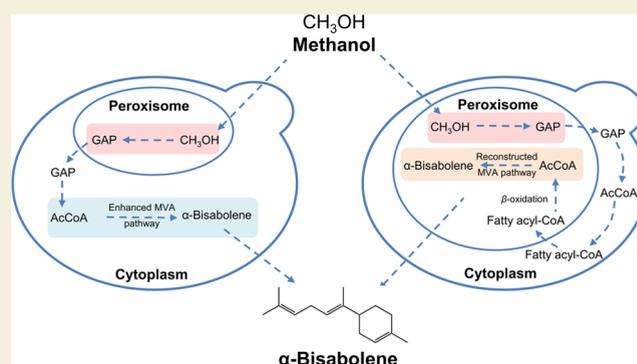
Metrics & More

Article Recommendations

Supporting Information

**ABSTRACT:** Microbial metabolic engineering provides a feasible approach to sustainably produce advanced biofuels and biochemicals from renewable feedstocks. Methanol is an ideal feedstock since it can be massively produced from CO<sub>2</sub> through green energy, such as solar energy. However, engineering microbes to transform methanol and overproduce chemicals is challenging. Notably, the microbial production of isoprenoids from methanol is still rarely reported. Here, we extensively engineered *Pichia pastoris* (syn. *Komagataella phaffii*) for the overproduction of sesquiterpene  $\alpha$ -bisabolene from sole methanol by optimizing the mevalonate pathway and peroxisomal compartmentalization. Furthermore, through label-free quantification (LFQ) proteomic analysis of the engineered strains, we identified the key bottlenecks in the peroxisomal targeting pathway, and overexpressing the limiting enzyme EfmvaE significantly improved  $\alpha$ -bisabolene production to 212 mg/L with the peroxisomal pathway. The engineered strain LH122 with the optimized peroxisomal pathway produced 1.1 g/L  $\alpha$ -bisabolene under fed-batch fermentation in shake flasks, achieving a 69% increase over that of the cytosolic pathway. This study provides a viable approach for overproducing isoprenoid from sole methanol in engineered yeast cell factories and shows that proteomic analysis can help optimize the organelle compartmentalized pathways to enhance chemical production.

**KEYWORDS:** methanol biotransformation, metabolic engineering, proteomic analysis, sesquiterpene, *Pichia pastoris*



## INTRODUCTION

Isoprenoids are widely applied in cosmetics, food additives, and pharmaceuticals and possess a high market value. Bisabolene, a monocyclic sesquiterpene compound, emits a distinct aroma and exhibits anti-inflammatory and antioxidant properties. Moreover, its hydrogenation product, bisabolane, serves as a substitute for D2 diesel.<sup>1,2</sup> Available resources to extract bisabolenes from their natural producers are limited, and microbial production is a feasible approach to generate a sustainable supply.<sup>1,3–5</sup> By optimizing the biosynthetic pathway and rewiring the cellular metabolism, several microbes have been harnessed for the production of a variety of isoprenoids from sugar.<sup>6–10</sup> With the increasing demand for biochemical production, the sugar supply might suffer due to limited arable land and competition with the food supply.

Methanol, an important chemical feedstock,<sup>11</sup> can be produced from natural gas and CO<sub>2</sub> by using green energy, such as solar energy.<sup>12</sup> Thus, sustainable chemical production can be achieved in a carbon-neutral manner through the biotransformation of methanol, which generates high-value and complex molecules.<sup>13–16</sup> *Pichia pastoris* (also known as

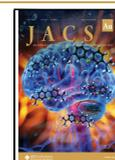
*Komagataella phaffii*) is a methylotrophic yeast that has been used to produce various proteins.<sup>17,18</sup> Compared with the production of valued proteins, chemical overproduction requires extensive metabolic rewiring to drive the metabolic flux toward target molecules. Although the rapid development in genetic tools facilitates the metabolic engineering of *P. pastoris*,<sup>19–21</sup> engineering *P. pastoris* for chemicals overproduction from sole methanol remains challenging because the process of metabolizing methanol is complex and relatively unclear. In previous studies, nutrient-rich medium or additional carbon sources such as glucose are often required to increase the titer of target chemicals or to improve cell growth during methanol biotransformation,<sup>22,23</sup> which at the same

Received: February 2, 2024

Revised: March 8, 2024

Accepted: March 25, 2024

Published: April 29, 2024



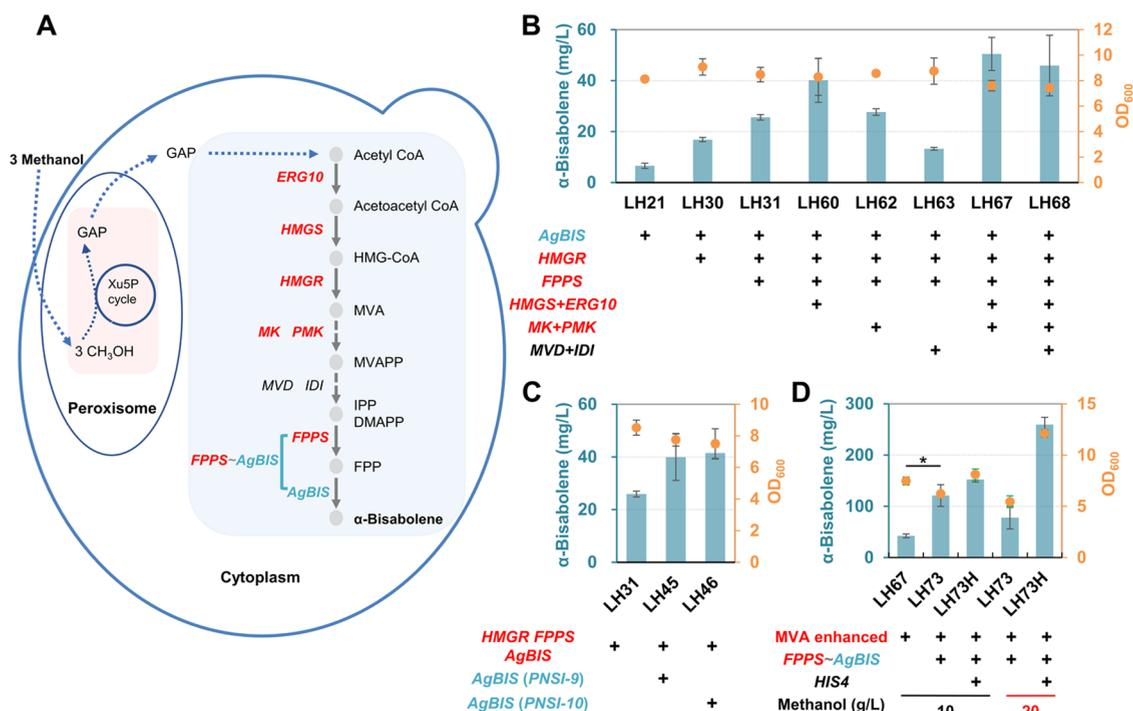


**Figure 1.** Optimization of the cytosolic MVA pathway for  $\alpha$ -bisabolene production from methanol in *P. pastoris*. (A) Schematic illustration of the optimized MVA pathway for  $\alpha$ -bisabolene biosynthesis from methanol. Overexpressed endogenous genes are shown in red, whereas heterologous genes are shown in blue. The dotted lines represent multiple enzyme reaction steps. The small curve between *FPPS* and *AgBIS* represents a flexible linker with the sequence “GGGS.” (B)  $\alpha$ -Bisabolene titers and cell densities of engineered strains in shake flasks after 120 h of cultivation at 220 rpm and 30 °C with 10 g/L methanol minimal medium. (C) Overexpression of the *AgBIS* gene at two different genomic integration sites. (D) *HIS4* complementation and higher methanol concentration (20 g/L) for improvement of  $\alpha$ -bisabolene production. Error bars represent the standard deviation (SD) of triplicate biological replicates. \* $P < 0.05$ .

time increases the production cost and the complexity of the cultivation process.

Here, we extensively engineered *P. pastoris* to overproduce  $\alpha$ -bisabolene by optimizing the mevalonate (MVA) pathway. We first optimized the cytosolic MVA pathway and expressed  $\alpha$ -bisabolene synthase, which improved  $\alpha$ -bisabolene production by 40-fold. To couple  $\alpha$ -bisabolene biosynthesis and methanol utilization, we reconstructed and optimized the MVA pathway in peroxisomes, which generated levels of  $\alpha$ -bisabolene (46%) much lower than those of the cytosolic pathway. Label-free quantification (LFQ) proteomic analysis revealed that acetoacetyl-CoA thiolase was a bottleneck in the peroxisomal MVA biosynthetic pathway and that overexpressing *EfMvaE* from *Enterococcus faecalis* significantly improved  $\alpha$ -bisabolene production by 72%. Fed-batch fermentation of the strain with the optimized peroxisomal pathway produced 1.1 g/L  $\alpha$ -bisabolene, which was 69% higher than that of the cytosolic pathway (0.67 g/L). This study described the comprehensive optimization of the MVA pathway for sesquiterpene overproduction from methanol and showed that proteomic analysis was helpful for identifying the bottleneck in the isoprenoid biosynthetic pathway, which might provide a feasible approach for optimizing the metabolic pathway to overproduce other chemicals in *P. pastoris*.

## RESULTS

### Engineering the Cytosolic MVA Pathway for $\alpha$ -Bisabolene Production from Methanol

We used the  $\alpha$ -bisabolene synthase gene *AgBIS* from *Abies grandis* for  $\alpha$ -bisabolene synthesis by catalyzing the conversion

of the cytosolic precursor FPP.<sup>24</sup> The *AgBIS* gene was codon-optimized according to the *P. pastoris* codon bias and integrated into the chromosome in strain PC110.<sup>19</sup> We used the strong promoter  $P_{DAS2}$  to express the *AgBIS* gene, which was helpful for draining the metabolic flux toward  $\alpha$ -bisabolene production. The engineered strain LH21 produced 6.6 mg/L in a shake flask containing 10 g/L methanol (Figures 1A,B and S1A–D). We also showed that rubber plugs were better than parafilm for shake flask fermentation with decreased methanol evaporation and increased  $\alpha$ -bisabolene production (Figure S2A–C).

We then tried to optimize the MVA pathway to improve  $\alpha$ -bisabolene biosynthesis. Overexpression of the 3-hydroxy-3-methylglutaryl-CoA (HMG-CoA) reductase gene *HMGR* (strain LH30) and farnesyl diphosphate synthase gene *FPPS* (strain LH31) resulted in increased production of  $\alpha$ -bisabolene to 16.8 and 25.6 mg/L, respectively. Further overexpression of the acetoacetyl-CoA thiolase gene *ERG10* and the HMG-CoA synthase gene *HMGS* improved  $\alpha$ -bisabolene production to 40.1 mg/L (strain LH60), and a small improvement in  $\alpha$ -bisabolene production (27.7 mg/L) was achieved by overexpressing the mevalonate kinase gene *MK* and the phosphomevalonate kinase gene *PMK* (strain LH62). Combinatorial overexpression of *ERG10*, *HMGS*, *MK*, and *PMK* further improved  $\alpha$ -bisabolene production to 50.5 mg/L. However, overexpression of the mevalonate-5-diphosphate decarboxylase gene *MVD* and the IPP isomerase gene *IDI* had a negative effect on  $\alpha$ -bisabolene production (strain LH63 vs LH31), suggesting that these corresponding reactions were not the limiting step for isoprenoid biosynthesis. Alternatively,

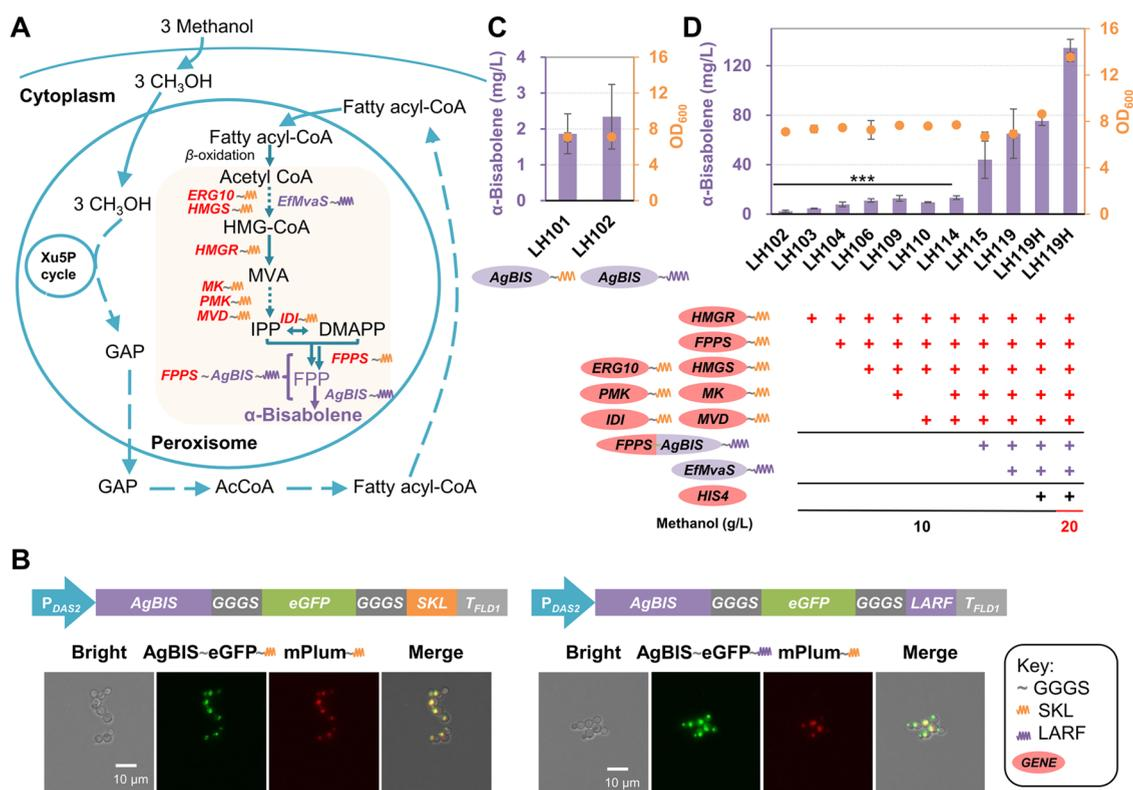


**Figure 2.** Reconstruction of MVA pathway in peroxisomes. (A) Schematic illustration of the reconstructed MVA pathway in peroxisomes. Overexpressed endogenous genes are displayed in red, while heterologous genes are shown in purple. The dotted lines represent multiple enzyme reaction steps. The C-terminal of all genes involved in the peroxisomal engineering pathway was fused with the peroxisome signal peptide “SKL” (which was shown to be an orange curve) or “LARF” (which was shown to be a purple curve). (B) Fluorescence analysis of the localization of AgBis fused to the peroxisome signal peptide by fluorescence microscopy. AgBis was fused with eGFP and the peroxisome signal peptide “SKL” or “LARF”. (C)  $\alpha$ -Bisabolene production and cell densities of overexpressing AgBis with the peroxisome signal peptide “SKL” or “LARF.” (D)  $\alpha$ -Bisabolene production and cell densities of engineered strains with the peroxisomal MVA pathway. The engineered strains were cultivated in shake flasks containing minimal medium with 10 g/L methanol or 20 g/L methanol for 120 h at 220 rpm and 30 °C. Error bars represent the SD of triplicate biological replicates. \*\*\* $P < 0.001$ .

overexpression of another copy of the *AgBIS* gene at two different genomic integration sites<sup>19</sup> improved  $\alpha$ -bisabolene production by 56 and 62%, respectively (Figure 1C), suggesting that the driving FPP flux to sesquiterpene synthase was beneficial for  $\alpha$ -bisabolene biosynthesis.

We thus enhanced the conversion of FPP toward  $\alpha$ -bisabolene synthesis in strain LH67 with the integration of *CAS9*, which simplified the construction of gRNA-expressing plasmids<sup>19</sup> and had no impact on cell growth and  $\alpha$ -bisabolene production (Figure S3A,B). To facilitate the substrate channeling of FPP toward AgBis, we overexpressed a fusion gene, *FPPS-AgBIS*, encoding a fusion enzyme of Fpps and AgBis, which significantly improved  $\alpha$ -bisabolene production by 2.8-fold (strain LH73, Figure 1D). We then evaluated the performance of strain LH73 under a higher methanol concentration of 20 g/L; however, cell growth was retarded and  $\alpha$ -bisabolene production decreased (Figure 1D). Stepwise addition of 10 g/L methanol (10 + 10 g/L) at 24, 48, and 72 h could alleviate methanol toxicity; however, the improvement in  $\alpha$ -bisabolene production was marginal compared with that with 10 g/L methanol (Figure S4). We previously observed that auxotrophs compromise cell growth and fatty acid production from glucose in *Saccharomyces cerevisiae*.<sup>25</sup> And methanol metabolism requires expressing high amounts of methanol-related enzymes in *P. pastoris*,<sup>26</sup> which suggests that amino acid nutrient deficiency might be the rate-limiting step

for the growth of the strain. We thus tried to restore the *HIS4* gene in the *his4* $\Delta$  mutant strain LH73, and an improvement in  $\alpha$ -bisabolene production was achieved with the resulting strain LH73H compared to LH73 under 10 g/L methanol (Figure 1D). Cultivating the strain LH73H in 20 g/L methanol achieved better cell growth and a much higher  $\alpha$ -bisabolene titer (260 mg/L) compared with that of 10 g/L methanol (152 mg/L, Figure 1D), suggesting that *HIS4* or histidine played an important role in methanol tolerance and cell growth.<sup>25</sup>

### Reconstruction of the MVA Pathway in the Peroxisome

Peroxisomes are organelles that perform methanol oxidation and fatty acid  $\beta$ -oxidation and contain sufficient acetyl-CoA.<sup>27,28</sup> Thus, reconstructing the MVA pathway in peroxisomes might be beneficial for isoprenoid production by eliminating side-pathway competition and coupling to methanol utilization (Figure 2A). The peroxisome signal peptides SKL and LARF<sup>29,30</sup> were used to target MVA enzymes into peroxisomes in strain PC110. Fusing the fluorescent protein and  $\alpha$ -bisabolene synthase AgBis showed that these signal peptides were functional for peroxisomal targeting (Figures 2B and S5A–D). Peroxisomal targeting of AgBis resulted in a small amount of  $\alpha$ -bisabolene production, and LARF (2.3 mg/L) was better than SKL (1.9 mg/L) for  $\alpha$ -bisabolene production (Figure 2C). This lower  $\alpha$ -bisabolene production might be attributed to the insufficient supply of

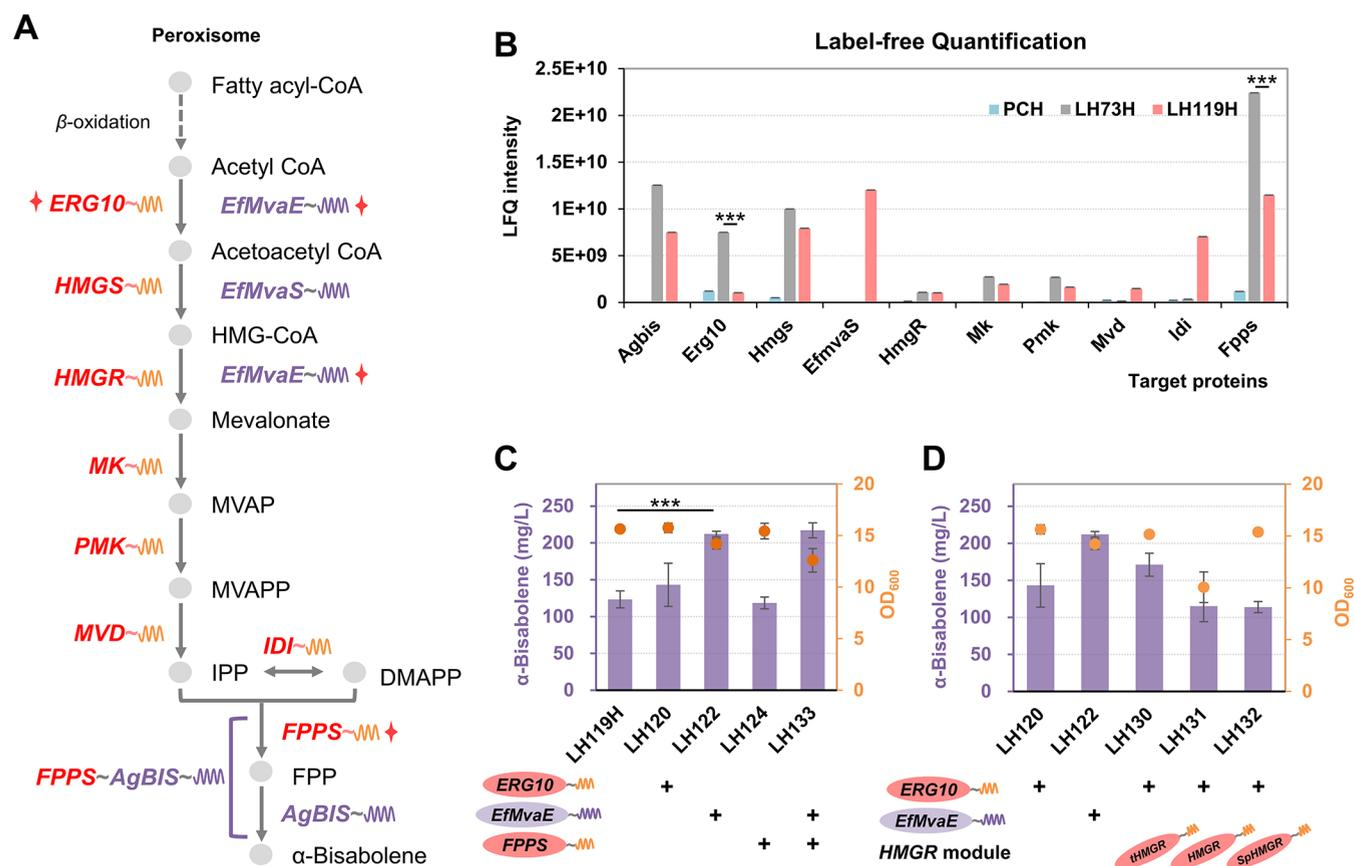


**Figure 3.** LFQ proteomic analysis of peroxisomal MVA pathway strain LH119H compared with LH73H and the wild-type strain PCH. (A) Scheme of the engineered peroxisome pathway. Overexpressed endogenous genes are displayed in red, while heterologous genes are shown in purple. The dotted lines represent multiple enzyme reaction steps. The C-terminal of all genes involved in the peroxisomal engineering pathway was fused with the peroxisome signal peptide “SKL” (which was shown to be an orange curve) or “LARF” (which was shown to be a purple curve). The genes with red stars are the rate-limiting targets for LH119H compared to LH73H. (B) Quantification of MVA enzymes compared with strains PCH, LH73H, and LH119H. (C) Overexpressing the limiting enzymes for  $\alpha$ -bisabolene production in LH119H. (D) Comparison of the expression of *EfmvaE* and different versions of *HMGR* for  $\alpha$ -bisabolene production. *tHMGR*, truncated *HMGR* with removing the amino acid 2 (Leu)-500 (His); *SpHMGR*: codon-optimized *HMGR* from *Silicibacter pomeroyi*. The engineered strains were cultivated in shake flasks containing minimal medium with 20 g/L methanol for 120 h at 220 rpm and 30 °C. Error bars represent the SD of triplicate biological replicates. \*\*\**P* < 0.001.

precursors, such as FPP, because the MVA pathway in the peroxisomes was incomplete.

We then tried to target the enzymes of the MVA pathway in peroxisomes, which significantly improved  $\alpha$ -bisabolene production (Figure 2D). Through reconstructing the complete MVA pathway in peroxisomes (strain LH114), 5.7-fold higher  $\alpha$ -bisabolene production was achieved than that of strain LH102 with only *AgBIS* expression (Figure 2D). Further overexpressing a fusion gene *FPPS-AgBIS* improved  $\alpha$ -bisabolene production by 3.3-fold (strain LH115 vs LH114, Figure 2D), which was similar to that of the cytosolic pathway. However, the  $\alpha$ -bisabolene titer (44.0 mg/L) in strain LH115 was much lower than that in strain LH73 (121 mg/L) with a cytosolically optimized MVA pathway. It has been reported that bifunctional acetoacetyl-CoA thiolase/HMG-CoA reductase (*EfmvaE*) and 3-hydroxy-3-methylglutaryl-Coenzyme A (HMG-CoA) synthase (*EfmvaS*) catalyze consecutive steps of mevalonate biosynthesis from acetyl-CoA.<sup>27</sup> Overexpression of *EfmvaS* (strain LH119) improved  $\alpha$ -bisabolene production to 65.1 mg/L, which was 48% higher than that of the control strain LH115 (Figure 2D). However, expression of *EfmvaE* in the genome has been attempted but failed when cointegrating with *EfmvaS* into genome. Again, complementing the *HIS4*

gene slightly improved  $\alpha$ -bisabolene biosynthesis from 10 g/L methanol and led to 134 mg/L  $\alpha$ -bisabolene production from 20 g/L methanol as a sole carbon source (Figure 2D).

### Proteome-Guided Engineering of Peroxisomal Biosynthetic Pathway

As a lower production of  $\alpha$ -bisabolene was achieved through the peroxisomal pathway (LH119H) than the cytosolic pathway (LH73H), the reconstructed peroxisomal pathway may include limiting steps. We thus performed comparative proteomic analysis of the engineered isoprenoid biosynthetic pathway (Figure 3A,B) in LH119H, LH73H, and the wild-type strain PCH. The engineered strains LH119H and LH73H contained much higher protein levels of the MVA pathway than the wild-type strain (Figure 3B). Most enzymes of the MVA pathway, except *Mvd* and *Idi*, were expressed at higher levels in LH73H than in LH119H. *Erg10* and *Fpps* levels were much higher in LH73H than in LH119H. Moreover, the *EfmvaE* protein was not detected in the peroxisome-modified strain LH119H, suggesting the failure to express *EfmvaE*. The low expression of MVA enzymes might be the bottleneck for the peroxisomal production of  $\alpha$ -bisabolene.

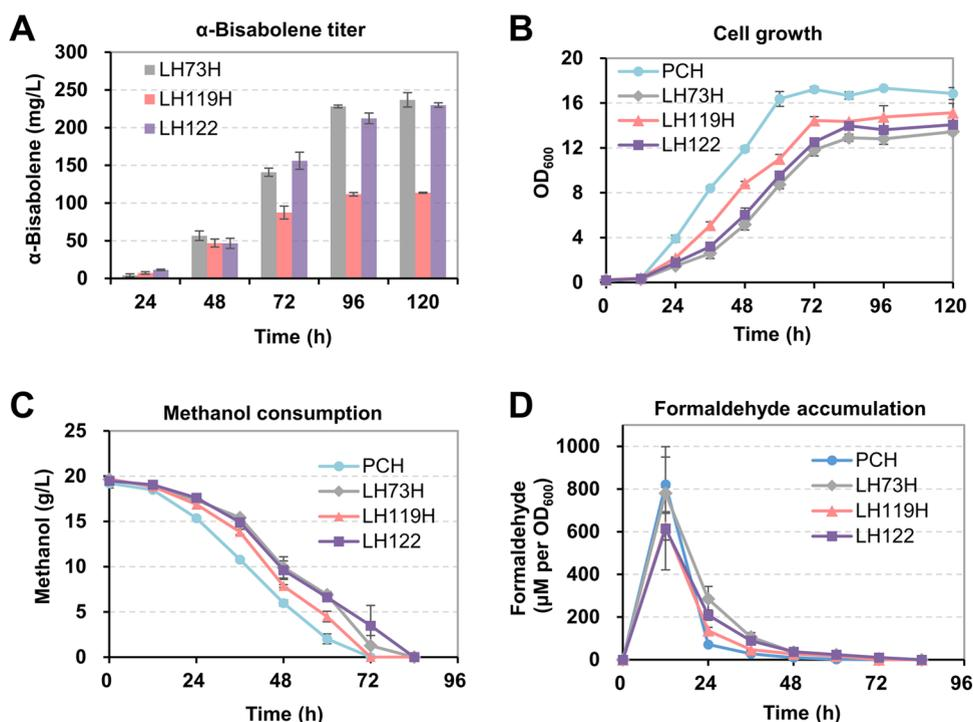


**Figure 4.** Evaluation of the engineered strains LH73H, LH119H, LH122, and the wild-type strain PCH under batch fermentation in shake flasks. (A)  $\alpha$ -Bisabolene production. (B) Cell growth. (C) Methanol consumption. (D) Formaldehyde accumulation. The engineered strains were cultivated at 220 rpm and 30 °C with 20 g/L methanol minimal medium. Error bars represent the SD of triplicate biological samples.

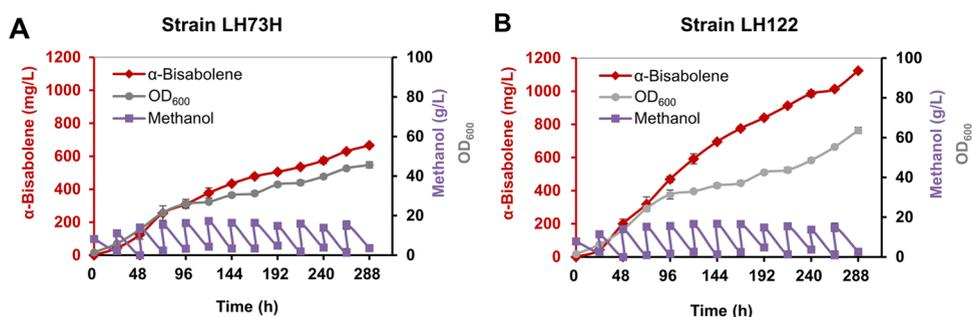


**Figure 5.** Fed-batch fermentation of LH73H and LH122 in shake flasks. Time courses of cell growth,  $\alpha$ -bisabolene titers, and methanol consumption of LH73H (A) and LH122 (B). Error bars represent the SD of triplicate biological samples.

We then tried to integrate another copy of *ERG10*, *EfMvaE*, and *FPPS* for  $\alpha$ -bisabolene production, which showed that overexpression of peroxisomal *EfMvaE* protein significantly increased the  $\alpha$ -bisabolene titer to 212 mg/L (Figure 3C), a 72% improvement compared to that of the control strain LH119H. These results suggested that functional expression of *EfMvaE* was essential to drive the metabolic flux toward isoprenoid biosynthesis in peroxisomes. Further overexpressing another copy of *FPPS* slightly increased  $\alpha$ -bisabolene production with reduced final biomass (Figures 3C and S6). It was reported that *EfmvaE* is a bifunctional enzyme of acetoacetyl-CoA thiolase/HMG-CoA reductase and is equivalent to endogenous *Erg10* and *HmgR*.<sup>27</sup> Although the protein level of *HmgR* in LH119H was equivalent to that of LH73H, *HmgR* was untruncated and might be inefficient. We thus tried to overexpress *ERG10* and different versions of *HMGR*.<sup>9,31,32</sup> It was shown that overexpression of *ERG10* and truncated *HMGR* slightly improved  $\alpha$ -bisabolene production; however, the improvement was much less than that of *EfMvaE* overexpression (Figure 3D). These results suggested that

*EfmvaE* expression helped drive the metabolic flux toward  $\alpha$ -bisabolene biosynthesis by enhancing the first MVA step of acetoacetyl-CoA thiolation.

#### Profiling the Engineered Strains in Shake Flasks

We evaluated the performances of the cytosol engineering strain LH73H, the peroxisome engineering strains LH119H and LH122, and the wild-type strain PCH under batch fermentation in shake flasks. Compared to the strain LH119H with failed expression of *EfMvaE*, the peroxisomal pathway optimized strain LH122 exhibited a much higher  $\alpha$ -bisabolene titer (Figure 4A). These data indicated that enhancing the upper part of the MVA pathway (overexpression of *EfMvaE*) was beneficial for the utilization of acetyl-CoA and the synthesis of sesquiterpene in the peroxisome engineering strains. The cell growth of  $\alpha$ -bisabolene-producing strains LH73H, LH119H, and LH122 was slower than that of the wild-type strain PCH (Figure 4B), suggesting that engineering  $\alpha$ -bisabolene biosynthesis brought a metabolic burden to cellular fitness. Peroxisomal overexpression of *EfMvaE*

retarded cell growth as well as methanol consumption (strain LH122 vs LH119H, Figure 4B,C). Interestingly, formaldehyde accumulation in peroxisome-engineered strains was lower than that of the wild-type strain and the cytosolic MVA pathway strain (Figure 4D), which suggested that engineering isoprenoid biosynthesis in peroxisomes was helpful for formaldehyde assimilation.

### Fed-Batch Fermentation

We finally compared the performance of the final peroxisomal-engineered strain LH122 and cytosol-engineered strain LH73H under fed-batch fermentation in a shake flask. These two strains exhibited similar methanol consumption capacities. However, LH122 produced 1124 mg/L  $\alpha$ -bisabolene at 288 h, with a yield of 7.6 mg/g (2.9% of theoretical yield), which was 1.7-fold greater than that of strain LH73H, and strain LH122 exhibited better growth than strain LH73H (Figure 5A,B). Since the MVA biosynthesis genes were overexpressed with methanol-inducible promoters (Table S1), peroxisomal compartmentalization of MVA pathways might be helpful for coupling isoprenoid biosynthesis and methanol assimilation. The better performance attained using fed-batch fermentation compared with batch fermentation might be explained by the constant boost in peroxisome biogenesis generated through methanol feeding; in contrast, batch fermentation might have exhausted methanol and the corresponding reduced peroxisomes. These observations remind us that we should carefully evaluate our engineered strains under different conditions by considering the differences in methanol metabolism and glucose metabolism.

### DISCUSSION

Although *P. pastoris* has been widely used as a cell factory for the production of a variety of compounds,<sup>33–35</sup> engineering the overproduction of complex secondary metabolites, such as isoprenoids, from sole methanol remains challenging. Here, we comprehensively optimized the MVA pathway in the peroxisome and cytosol for the overproduction of sesquiterpene.

The peroxisome is an ideal organelle for biosynthesis with several advantages, for example, enzymes and precursors are present at high concentrations, the loss of intermediates is low, and toxic enzymes or intermediates are insulated.<sup>28,30,36–39</sup> In these studies, peroxisomes were harnessed for chemical overproduction from glucose without greatly damaging cellular fitness since peroxisomes are relatively nonessential under glucose cultivation. Information about engineering complex biosynthetic pathways in peroxisomes by using methanol as a sole carbon source is limited. Furthermore, there is no systematic comparison of the performance between cytosolic and peroxisomal biosynthetic pathways, as previous studies only compared the initial pathways.<sup>40</sup> Here, we comprehensively optimized the MVA pathways in the cytosol and peroxisome and compared their performance for  $\alpha$ -bisabolene production under batch and fed-batch fermentations in shake flasks. The optimized peroxisomal pathway generated much higher levels of  $\alpha$ -bisabolene than the cytosolic pathway under fed-batch fermentation, while similar  $\alpha$ -bisabolene production was observed under batch fermentation. Continuous methanol feeding might be helpful for peroxisomal proliferation<sup>41</sup> and thus stimulate the peroxisomal MVA pathways for  $\alpha$ -bisabolene production.

Identifying bottlenecks of biosynthetic pathways remains a challenge, and proteomics might be helpful for identifying bottlenecks that compromise biosynthetic efficiency.<sup>42,43</sup> Here, we compared the LFQ proteome of the MVA pathway between the engineered peroxisomal and cytosolic pathways, which revealed that the first step of acetoacetyl-CoA thiolase was a bottleneck in the peroxisomal biosynthetic pathway. This observation shows that comparative LFQ proteomics is a feasible approach to guide pathway optimization.<sup>27</sup>

In summary, we comprehensively optimized and compared the MVA pathway in the peroxisome and cytosol to produce sesquiterpene  $\alpha$ -bisabolene from the sole methanol in *P. pastoris*. Though the  $\alpha$ -bisabolene production from methanol was lower than that from glucose,<sup>1,3–5</sup> further engineering central metabolism<sup>33,35</sup> and enhancing the methanol tolerance<sup>44,45</sup> should be helpful for improving the cellular performance for chemical production.

### METHODS

#### Strains and Media

All strains used in this study are listed in Table S1. *Escherichia coli* DH5 $\alpha$  was used for plasmid propagation. PC110 derived from GS115 with a *RAD52*-expressing cassette at the *HIS4* site constructed in our previous study<sup>19</sup> was used as the parent strain for  $\alpha$ -bisabolene biosynthesis. The engineering strategy and flowcharts of yeast strain construction are shown in Figures S7 and S8.

The Luria–Bertani (LB) broth medium (10 g/L NaCl, 10 g/L tryptone, 5 g/L yeast extract) with 100 mg/L ampicillin or 50 mg/L kanamycin was used for the growth of *E. coli*, which were cultured at 37 °C with shaking at 220 rpm. The YNB medium (20 g/L glucose and 6.7 g/L yeast nitrogen base without amino acids) with essential nutrients for yeast cultivation and the yeast culture were incubated at 30 °C with shaking at 220 rpm. YPD medium (20 g/L glucose, 20 g/L peptone, 10 g/L yeast extract) containing 100 mg/L Zeocin or 200 mg/L Geneticin was used to cultivate yeast strain containing gRNA-expressing plasmids. Solid medium was added to 15 g/L Agar. Minimal medium (MM) (2.5 g/L (NH<sub>4</sub>)<sub>2</sub>SO<sub>4</sub>, 14.4 g/L KH<sub>2</sub>PO<sub>4</sub>, 0.5 g/L MgSO<sub>4</sub>·7H<sub>2</sub>O, and 4 M KOH were added to adjust the pH value 5.6, 1 mL/L vitamin solution, 2 mL/L trace metal solution), containing 10 or 20 g/L methanol as carbon sources, was used to produce  $\alpha$ -bisabolene in shake flasks. For the fermentation of the *his4* $\Delta$  mutant strains, 40 mg/L of histidine was added to the minimal medium. When conducting fed-batch fermentation, 9–14 g/L methanol and 0.4 mL feeding culture containing 10 $\times$  delft media were supplemented every 24 h.

#### DNA Manipulation

All of the primers used in this study are listed in Table S2. The coding sequences of  $\alpha$ -bisabolene synthase (*AgBIS*; GenBank accession no. AF006195.1) from *A. grandis*, 3-hydroxy-3-methylglutaryl-Coenzyme A (HMG-CoA) synthase (*EfMvaS*; GenBank accession no. KX064238), and bifunctional acetoacetyl-CoA thiolase/HMG-CoA reductase (*EfMvaE*; GenBank accession no. KX064239) from *E. faecalis* were codon-optimized and synthesized by GENEWIZ Corporation (Suzhou, China) (Table S3). Genomic DNA from the *P. pastoris* strain was extracted using the E.Z.N.A. Yeast DNA Kit (Omega Bio-Tek Inc.). All endogenous genes involved in the MVA pathway were polymerase chain reaction (PCR)-amplified from the genomic DNA of *P. pastoris* using Phanta Super-Fidelity DNA Polymerase (Vazyme, Nanjing, China).

The pCAI plasmid was used as the template for the construction of all gRNA-expressing plasmids as described previously.<sup>19</sup> Donor DNA fragments containing the expressing gene and the homologous arms were prepared via fusion PCR<sup>46</sup> by using corresponding primers listed in Table S2 and then transformed to *P. pastoris* strains.<sup>19</sup> For gene overexpression, an expression cassette containing a promoter, a gene, and a terminator was amplified via PCR, respectively, and constructed

into one fragment through fusion PCR. The yeast cells were selected on YPD with 200  $\mu\text{g}/\text{mL}$  G418 plates and then were subjected to colony PCR. To remove the plasmids for the next round of genetic manipulation, the transformants were cultured in the YPD medium for 24 h twice and then plated onto YPD plates for 4 days.

### Proteomic Analysis

Samples of PCH, LH73H, and LH119H were cultivated according to the culture method of shake flask cultivation and then collected for protein extraction. 10–20 mg (dry cell weight) yeast cells was collected in the logarithmic stage (33 h for PCH, 47 h for LH73H, 37 h for LH119H). Yeast cell pellets were homogenized with 0.4 mm glass beads by using a 3D-freezing grinder (Servicebio, Wuhan, China) for 10 repeated 40 s cycles at 6 m/s, with a 60 s pause. The lysate was transferred to new tubes and diluted 10 times with the lysis buffer. The protein concentration was determined by using the Bradford Assay Kit. All lysis buffers were added with a 1% (v/v) protease inhibitor cocktail. Samples of yeast cell pellets were treated in triplicate using an ionic liquid-based filter-aided sample preparation (i-FASP) method.<sup>47</sup> In brief, samples were incubated at 95 °C for 3 min and another 30 min at room temperature. The cell debris was removed by centrifugation at 16,000g at 4 °C for 5 min, and 100–150  $\mu\text{g}$  of the clarified protein extract was transferred to a 10 kDa filter. After centrifugation on the filter at 14,000g at 20 °C for 15 min, the extracted proteins were retained, diluted with 200  $\mu\text{L}$  of 50 mM  $\text{NH}_4\text{HCO}_3$ , and centrifuged again at 14,000g at 20 °C for 15 min. Subsequently, 200  $\mu\text{L}$  of 50 mM IAA was dissolved in 50 mM  $\text{NH}_4\text{HCO}_3$  buffer, and the samples were incubated in darkness for 10 min. Then, the samplers were fileted, washed three times with 200  $\mu\text{L}$  of 50 mM  $\text{NH}_4\text{HCO}_3$ , and then digested overnight at 37 °C by adding 100  $\mu\text{L}$  of 10 mM  $\text{NH}_4\text{HCO}_3$  containing trypsin (3–6  $\mu\text{g}$ ). Finally, the tryptic peptides were collected by centrifugation, and 50  $\mu\text{L}$  of water was added to elute the peptide-rich solution twice. Peptides were extracted, vacuum-dried, and stored at –80 °C until LC-MS/MS analysis.

A nano-RPLC-ESI-MS/MS system was set up for quantitative proteomic analysis, which consists of an Orbitrap Exploris 480 instrument with a FAIMS Pro device and an Easy-nano LC 1200 system (ThermoFisher Scientific). Dried peptides were resuspended to 1  $\mu\text{g}/\mu\text{L}$  using 0.1% FA and separated by a C18 capillary column (150  $\mu\text{m}$  i.d.  $\times$  30 cm), which was packed in-house with ReproSil-Pur C18-AQ particles (1.9  $\mu\text{m}$ , 120 Å) and heated to 55 °C at a flow of 0.6  $\mu\text{L}/\text{min}$ . Mobile phase solvent A consisted of 0.1% FA in high-performance liquid chromatography (HPLC)  $\text{H}_2\text{O}$ , and mobile phase solvent B consisted of 0.1% FA in 80% acrylonitrile (ACN) and 20% HPLC  $\text{H}_2\text{O}$ . 65-min separation gradient was as follows: 0–45 min (12–30% B), 45–51 min (30–38% B), 51–55 min (38–95%), 55–59 min (95% B), and 59–65 min (95% B). FAIMS separations were performed with the following settings: inner and outer electrode temperature = 100 °C; total carrier gas = 4.0 L/min; CV values were –45 and –65 for each injection. The MS analysis was performed in data-dependent acquisition (DDA) mode with a resolution of 60,000 for MS1 scans from  $m/z$  350–1500 and 15,000 for MS2 scans with first mass at 110 and an isolation width of 1.6  $m/z$ . The target automatic gain control (AGC) was  $3 \times 10^6$  and  $7.5 \times 10^4$  ions for MS1 and MS2 scans, and the max injection time was 20 ms for MS1 and 30 ms for MS2 scans. The precursors with charge states of 2–7 with an intensity higher than 25,000 were selected for higher energy collisional dissociation (HCD) fragmentation, and the dynamic exclusion was set to 30 s. The normalized HCD collision energy was set as 30%. The protein mass spectrometry raw data was deposited to ProteomeXchange (<http://www.proteomexchange.org>) with the accession number PXD048269. Raw datafiles were splitted to –45 and –65 V at first. Then, split raw datafiles were analyzed using MaxQuant (version 2.2.0.0) and searched against the *P. pastoris* GS115 reference proteome database downloaded from UniProt<sup>48</sup> (UP000000314; 5073 sequences; 20210226) and supplemented with GQ68\_03479T0 (AOA69352.1; NCBI), which frequently observed contaminants. The parameters were set as follows: MS1 tolerance of 10 ppm; MS2 mass tolerance of 20 ppm; enzyme specificity was set as

trypsin with a maximum of two missed cleavages allowed; carbamidomethylation of cysteine was set as a fixed modification (+57.02 Da); acetylation on the protein N-terminal (+42.01 Da) and oxidation of methionine (+15.99 Da) were set as variable modifications. The required false discovery rate (FDR) was set to 1% at both the peptide and the protein level, and the minimum required protein length was set at 7. At least two peptides were required for protein identification of which at least one peptide was required to be unique in the database. Identified proteins were quantified with MaxQuant's LFQ algorithm.<sup>49</sup> All of the label-free protein quantification among different samples was processed with Z-score normalization and multiple-sample tests (Benjamini–Hochberg FDR correction threshold of 0.05) with Perseus version 2.0.7.0 (<http://www.perseus-framework.org>).<sup>50</sup> The log<sub>2</sub> fold change (log<sub>2</sub>FC) data, which was greater than 1 or less than –1 in three biological replicates for the multiple-sample tests of each of the two samples, were assigned to differentially expressed proteins. The protein quantification between the samples was performed as previously described with some modification.<sup>51</sup>

### Fluorescence Microscopy Analysis

To confirm peroxisome targeting, the green fluorescent protein eGFP was fused to the C-terminal of  $\alpha$ -bisabolene synthase using the flexible linker GGGs, and the peroxisome localization signal peptide SKL or LARF was further fused to the C-terminal of eGFP (encoding gene *AgBIS* ~ *eGFP* ~ SKL or *AgBIS* ~ *eGFP* ~ LARF). Similarly, the peroxisome localization signal peptide SKL was fused to the C-terminal of mPlum (encoding gene *mPlum* ~ SKL), and then, the cassettes were transformed into the yeast strain PC111. The strain was incubated for 36 h at 220 rpm at 30 °C in MM medium containing 10 g/L methanol. Three microliters of the cell cultures was dropped onto the microscope slides, covered with the cover glass, and then observed the fluorescence display position with the EVOS M5000 microscope (ThermoFisher Scientific).

### Batch and Fed-Batch Fermentations in Shake Flasks

The yeast strains were cultivated at 30 °C and 220 rpm in a shake incubator (Zhichu ZQZY-CS8) to an initial optical density ( $\text{OD}_{600}$ ) of 0.2. The preculture was cultivated in a 15 mL tube with a working volume of 2 mL of YPD for 16 to 18 h. Then, the preculture cells were then washed with minimal medium and inoculated to 20 mL delft minimal medium containing 10 or 20 g/L methanol as carbon sources for 120 h in rubber plugs, and 2 mL of *n*-dodecane was added for production extraction with caryophyllene as an internal standard. Fed-batch fermentations in shake flasks were performed as follows: prototrophic strains were precultured in YPD for 16–18 h and then washed with minimal medium, which was subsequently transferred into 20 mL of delft minimal medium containing 10 g/L methanol with an initial  $\text{OD}_{600}$  of 1. After 24 h of cultivation, 9–14 g/L methanol and 0.4 mL of concentrated (10 $\times$ ) delft minimal medium were supplemented every 24 h. The pH was adjusted to approximately 5–6 with 4 M KOH based on pH test strips every 24 h. The cell density  $\text{OD}_{600}$  and the concentration of methanol were measured every 24 h by using a spectrophotometer and a SBA-40D biosensor (Biology Institute of Shandong Academy of Sciences), respectively. Three biologically independent samples were analyzed during the fermentation.

### Extraction and Quantification of $\alpha$ -Bisabolene

The dodecane phase of the cell culture was collected and subsequently subjected to gas chromatography (GC) to analyze the  $\alpha$ -bisabolene concentration using caryophyllene as an internal standard. The GC (Thermo Scientific TRACE 1300) was equipped with a flame ionization detector (FID) and an HP-5 column (30 m  $\times$  0.320 mm  $\times$  0.25  $\mu\text{m}$ ) with a flow rate of 1.0 mL/min. The injection volume was 1.0  $\mu\text{L}$  with a split ratio of 15, and the temperature of the injector and GC interface was 250 °C. The initial temperature was 60 °C, followed by a ramp to 200 °C at a rate of 40 °C/min and holding at 200 °C for 5 min.

## Quantification of Methanol and Formaldehyde

Yeast cell samples were taken every 12 h to analyze biomass ( $OD_{600}$ ), methanol, and formaldehyde. The methanol concentration was measured by high-performance liquid chromatography (HPLC). 0.2 mL of broth sample was centrifuged at 12,000g for 5 min, filtered through a 0.2  $\mu$ m syringe filter, and analyzed with an Aminex HPX-87H column (Bio-Rad) on an HPLC (LC-2030, Shimadzu, Japan) equipped with a differential refractive index detector. The column was eluted with 5 mM  $H_2SO_4$  at a flow rate of 0.6 mL/min at 50 °C for 25 min.

To measure formaldehyde, 0.04 mL of cell culture was mixed with 0.1 mL of 20% (w/v) trichloroacetic acid, 0.05 mL of 2,4-dinitrophenylhydrazine (DNPH) (1 g/L in acetonitrile), and 0.25 mL of acetonitrile and vortex vigorously for 1 min. The mixture was then incubated at 60 °C for 30 min and centrifuged at 12,000g for 5 min. The supernatant was filtrated through a 0.2  $\mu$ m syringe filter and analyzed using the HPLC equipped with a C18 reversed-phase column (Supersil ODS2, 2.1  $\times$  150 mm<sup>2</sup>, Dalian Yilite). 65% acetonitrile (65%) was used as the mobile phase with a flow rate of 0.3 mL/min. Formaldehyde-2,4-dinitrophenylhydrazine was quantified using a UV detector at 355 nm and 35 °C.

### Statistical Analysis

Statistical analysis was performed using Microsoft Excel software using a two-tailed *t* test analysis of the variance hypothesis. Significant differences are marked as \**P* < 0.05, \*\**P* < 0.01, and \*\*\**P* < 0.001. All data are presented as the means  $\pm$  SD. The number of biologically independent samples for each panel was three.

## ■ ASSOCIATED CONTENT

### Data Availability Statement

The protein mass spectrometry raw data was deposited to ProteomeXchange (<http://www.proteomexchange.org>) with the accession number PXD048269. All other data are available within the article and [Supporting Information](#) files.

### SI Supporting Information

The Supporting Information is available free of charge at <https://pubs.acs.org/doi/10.1021/jacsau.4c00106>.

Gas chromatograms; the comparison of plastic film and silicone plug; genome integration of CAS9; the fermentation of strain LH73; fluorescence analysis; cell growth of strain LH122 and LH133; flowchart of yeast strains' construction; strains (genotype description); primers; the sequence of optimized genes ([PDF](#))

## ■ AUTHOR INFORMATION

### Corresponding Authors

**Lihua Zhang** – Division of Biotechnology, Dalian Institute of Chemical Physics, Chinese Academy of Sciences, Dalian 116023, China; CAS Key Laboratory of Separation Science for Analytical Chemistry, Dalian Institute of Chemical Physics, Chinese Academy of Sciences, Dalian 116023, China; [orcid.org/0000-0003-2543-1547](https://orcid.org/0000-0003-2543-1547); Email: [lihuazhang@dicp.ac.cn](mailto:lihuazhang@dicp.ac.cn)

**Yongjin J. Zhou** – Division of Biotechnology, Dalian Institute of Chemical Physics, Chinese Academy of Sciences, Dalian 116023, China; Dalian Key Laboratory of Energy Biotechnology and CAS Key Laboratory of Separation Science for Analytical Chemistry, Dalian Institute of Chemical Physics, Chinese Academy of Sciences, Dalian 116023, China; [orcid.org/0000-0002-2369-3079](https://orcid.org/0000-0002-2369-3079); Email: [zhouyongjin@dicp.ac.cn](mailto:zhouyongjin@dicp.ac.cn)

## Authors

**Linhui Gao** – Division of Biotechnology, Dalian Institute of Chemical Physics, Chinese Academy of Sciences, Dalian 116023, China; Dalian Key Laboratory of Energy Biotechnology, Dalian Institute of Chemical Physics, Chinese Academy of Sciences, Dalian 116023, China; University of Chinese Academy of Sciences, Beijing 100049, China

**Rui Hou** – Division of Biotechnology, Dalian Institute of Chemical Physics, Chinese Academy of Sciences, Dalian 116023, China; University of Chinese Academy of Sciences, Beijing 100049, China; CAS Key Laboratory of Separation Science for Analytical Chemistry, Dalian Institute of Chemical Physics, Chinese Academy of Sciences, Dalian 116023, China

**Peng Cai** – Division of Biotechnology, Dalian Institute of Chemical Physics, Chinese Academy of Sciences, Dalian 116023, China; Dalian Key Laboratory of Energy Biotechnology, Dalian Institute of Chemical Physics, Chinese Academy of Sciences, Dalian 116023, China

**Lun Yao** – Division of Biotechnology, Dalian Institute of Chemical Physics, Chinese Academy of Sciences, Dalian 116023, China; CAS Key Laboratory of Separation Science for Analytical Chemistry, Dalian Institute of Chemical Physics, Chinese Academy of Sciences, Dalian 116023, China

**Xiaoyan Wu** – Division of Biotechnology, Dalian Institute of Chemical Physics, Chinese Academy of Sciences, Dalian 116023, China; Dalian Key Laboratory of Energy Biotechnology, Dalian Institute of Chemical Physics, Chinese Academy of Sciences, Dalian 116023, China; University of Chinese Academy of Sciences, Beijing 100049, China

**Yunxia Li** – Division of Biotechnology, Dalian Institute of Chemical Physics, Chinese Academy of Sciences, Dalian 116023, China; Dalian Key Laboratory of Energy Biotechnology, Dalian Institute of Chemical Physics, Chinese Academy of Sciences, Dalian 116023, China

Complete contact information is available at: <https://pubs.acs.org/doi/10.1021/jacsau.4c00106>

### Author Contributions

<sup>†</sup>L.G. and R.H. contributed equally to this work. All authors have given approval to the final version of the manuscript. CRediT: L.G.: conceptualization, investigation, data curation, visualization, and writing—original draft. R.H.: data curation, investigation, and methodology. P.C.: methodology and writing—review and editing. L.Y.: writing—review and editing. X.W.: methodology. Y.L.: methodology. L.Z.: writing—review and editing and supervision. Y.J.Z.: conceptualization, writing—review and editing, funding acquisition, and supervision.

### Funding

This research was supported by the National Key Research and Development Program of China (2022YFC2105900), Liaoning distinguished scholars (2023JH6/100500001), and DICP innovation grant (DICP I202335). Funding for open access charge: National Key Research and Development Program of China.

### Notes

The authors declare the following competing financial interest(s): Yongjin J. Zhou., Linhui Gao, Peng Cai, and Lun Yao have one patent for protecting part of the work described

herein. All other authors declare no competing financial interests.

## REFERENCES

- (1) Peralta-Yahya, P. P.; Ouellet, M.; Chan, R.; Mukhopadhyay, A.; Keasling, J. D.; Lee, T. S. Identification and microbial production of a terpene-based advanced biofuel. *Nat. Commun.* **2011**, *2*, No. 483.
- (2) Beller, H. R.; Lee, T. S.; Katz, L. Natural products as biofuels and bio-based chemicals: fatty acids and isoprenoids. *Nat. Prod. Rep.* **2015**, *32*, 1508–1526.
- (3) Zhao, Y.; Zhu, K.; Li, J.; Zhao, Y.; Li, S.; Zhang, C.; Xiao, D.; Yu, A. High-efficiency production of bisabolene from waste cooking oil by metabolically engineered *Yarrowia lipolytica*. *Microb. Biotechnol.* **2021**, *14*, 2497–2513.
- (4) Grenz, S.; Baumann, P. T.; Ruckert, C.; Nebel, B. A.; Siebert, D.; Schwentner, A.; Eikmanns, B. J.; Hauer, B.; Kalinowski, J.; Takors, R.; Blombach, B. Exploiting *Hydrogenophaga pseudoflava* for aerobic syngas-based production of chemicals. *Metab. Eng.* **2019**, *55*, 220–230.
- (5) Kim, E. M.; Woo, H. M.; Tian, T.; Yilmaz, S.; Javidpour, P.; Keasling, J. D.; Lee, T. S. Autonomous control of metabolic state by a quorum sensing (QS)-mediated regulator for bisabolene production in engineered *E. coli*. *Metab. Eng.* **2017**, *44*, 325–336.
- (6) Yang, H.; Zhang, K.; Shen, W.; Xia, Y.; Li, Y.; Chen, X. Boosting production of cembratriene-ol in *Saccharomyces cerevisiae* via systematic optimization. *Biotechnol. J.* **2023**, No. e2300324, DOI: 10.1002/biot.202300324.
- (7) Ke, X.; Pan, Z. H.; Du, H. F.; Shen, Y.; Shen, J. D.; Liu, Z. Q.; Zheng, Y. G. Secretory production of 7-dehydrocholesterol by engineered *Saccharomyces cerevisiae*. *Biotechnol. J.* **2023**, *18*, No. e2300056.
- (8) Paddon, C. J.; Westfall, P. J.; Pitera, D. J.; Benjamin, K.; Fisher, K.; McPhee, D.; Leavell, M. D.; Tai, A.; Main, A.; Eng, D.; Polichuk, D. R.; Teoh, K. H.; Reed, D. W.; Treynor, T.; Lenihan, J.; Fleck, M.; Bajad, S.; Dang, G.; Dengrove, D.; Diola, D.; Dorin, G.; Ellens, K. W.; Fickes, S.; Galazzo, J.; Gaucher, S. P.; Geistlinger, T.; Henry, R.; Hepp, M.; Horning, T.; Iqbal, T.; Jiang, H.; Kizer, L.; Lieu, B.; Melis, D.; Moss, N.; Regentin, R.; Secret, S.; Tsuruta, H.; Vazquez, R.; Westblade, L. F.; Xu, L.; Yu, M.; Zhang, Y.; Zhao, L.; Lievens, J.; Covello, P. S.; Keasling, J. D.; Reiling, K. K.; Renninger, N. S.; Newman, J. D. High-level semi-synthetic production of the potent antimalarial artemisinin. *Nature* **2013**, *496*, 528–532.
- (9) Meadows, A. L.; Hawkins, K. M.; Tsegaye, Y.; Antipov, E.; Kim, Y.; Raetz, L.; Dahl, R. H.; Tai, A.; Mahatdejkul-Meadows, T.; Xu, L.; Zhao, L.; Dasika, M. S.; Murarka, A.; Lenihan, J.; Eng, D.; Leng, J. S.; Liu, C. L.; Wenger, J. W.; Jiang, H.; Chao, L.; Westfall, P.; Lai, J.; Ganesan, S.; Jackson, P.; Mans, R.; Platt, D.; Reeves, C. D.; Saija, P. R.; Wichmann, G.; Holmes, V. F.; Benjamin, K.; Hill, P. W.; Gardner, T. S.; Tsong, A. E. Rewriting yeast central carbon metabolism for industrial isoprenoid production. *Nature* **2016**, *537*, 694–697.
- (10) Westfall, P. J.; Pitera, D. J.; Lenihan, J. R.; Eng, D.; Woolard, F. X.; Regentin, R.; Horning, T.; Tsuruta, H.; Melis, D. J.; Owens, A.; Fickes, S.; Diola, D.; Benjamin, K. R.; Keasling, J. D.; Leavell, M. D.; McPhee, D. J.; Renninger, N. S.; Newman, J. D.; Paddon, C. J. Production of amorphadiene in yeast, and its conversion to dihydroartemisinin acid, precursor to the antimalarial agent artemisinin. *Proc. Natl. Acad. Sci. U.S.A.* **2012**, *109*, E111–E118.
- (11) Tian, P.; Wei, Y. X.; Ye, M.; Liu, Z. M. Methanol to olefins (MTO): From fundamentals to commercialization. *ACS Catal.* **2015**, *5*, 1922–1938.
- (12) Shih, C. F.; Zhang, T.; Li, J.; Bai, C. Powering the future with liquid sunshine. *Joule* **2018**, *2*, 1925–1949.
- (13) Gao, J. Q.; Zhou, Y. J. Advances in methanol bio-transformation. *Synth. Biol. J.* **2020**, *1*, 158–173, DOI: 10.12211/2096-8280.2020-017.
- (14) Duan, X.; Gao, J.; Zhou, Y. J. Advances in engineering methylotrophic yeast for biosynthesis of valuable chemicals from methanol. *Chin. Chem. Lett.* **2018**, *29*, 681–686.
- (15) Zhou, Y. J.; Kerkhoven, E. J.; Nielsen, J. Barriers and opportunities in bio-based production of hydrocarbons. *Nat. Energy* **2018**, *3*, 925–935.
- (16) Wu, X. Y.; Cai, P.; Gao, L. H.; Li, Y. X.; Yao, L.; Zhou, Y. J. Efficient bioproduction of 3-hydroxypropionic acid from methanol by a synthetic yeast cell factory. *ACS Sustainable Chem. Eng.* **2023**, *11*, 6445–6453.
- (17) Gao, L. H.; Cai, P.; Zhou, Y. J. Advances in metabolic engineering of methylotrophic yeasts. *Chin. J. Biotechnol.* **2021**, *37*, 966–979, DOI: 10.13345/j.cjb.200645.
- (18) Yang, Z.; Zhang, Z. Engineering strategies for enhanced production of protein and bio-products in *Pichia pastoris*: A review. *Biotechnol. Adv.* **2018**, *36*, 182–195.
- (19) Cai, P.; Duan, X. P.; Wu, X. Y.; Gao, L. H.; Ye, M.; Zhou, Y. J. Recombination machinery engineering facilitates metabolic engineering of the industrial yeast *Pichia pastoris*. *Nucleic Acids Res.* **2021**, *49*, 7791–7805.
- (20) Vogl, T.; Sturmberger, L.; Kickenweiz, T.; Wasmayer, R.; Schmid, C.; Hatzl, A. M.; Gerstmann, M. A.; Pitzer, J.; Wagner, M.; Thallinger, G. G.; Geier, M.; Glieder, A. A toolbox of diverse promoters related to methanol utilization: Functionally verified parts for heterologous pathway expression in *Pichia pastoris*. *ACS Synth. Biol.* **2016**, *5*, 172–186.
- (21) Raschmanová, H.; Weninger, A.; Glieder, A.; Kovar, K.; Vogl, T. Implementing CRISPR-Cas technologies in conventional and non-conventional yeasts: Current state and future prospects. *Biotechnol. Adv.* **2018**, *36*, 641–665.
- (22) Luo, G.; Lin, Y.; Chen, S.; Xiao, R.; Zhang, J.; Li, C.; Sinskey, A. J.; Ye, L.; Liang, S. Overproduction of patchoulol in metabolically engineered *Komagataella phaffii*. *J. Agric. Food Chem.* **2023**, *71*, 2049–2058.
- (23) Liu, Y.; Tu, X.; Xu, Q.; Bai, C.; Kong, C.; Liu, Q.; Yu, J.; Peng, Q.; Zhou, X.; Zhang, Y.; Cai, M. Engineered monoculture and co-culture of methylotrophic yeast for de novo production of monacolin J and lovastatin from methanol. *Metab. Eng.* **2018**, *45*, 189–199.
- (24) Bohlmann, J.; Crock, J.; Jetter, R.; Croteau, R. Terpenoid-based defenses in conifers: cDNA cloning, characterization, and functional expression of wound-inducible (E)- $\alpha$ -bisabolene synthase from grand fir (*Abies grandis*). *Proc. Natl. Acad. Sci. U.S.A.* **1998**, *95*, 6756–6761.
- (25) Yan, C.; Gao, N.; Cao, X.; Yao, L.; Zhou, Y. J.; Gao, J. Auxotrophs compromise cell growth and fatty acid production in *Saccharomyces cerevisiae*. *Biotechnol. J.* **2023**, *18*, No. e2200510.
- (26) Liang, S.; Wang, B.; Pan, L.; Ye, Y.; He, M.; Han, S.; Zheng, S.; Wang, X.; Lin, Y. Comprehensive structural annotation of *Pichia pastoris* transcriptome and the response to various carbon sources using deep paired-end RNA sequencing. *BMC Genomics* **2012**, *13*, 738–751.
- (27) Dusséaux, S.; Wajn, W. T.; Liu, Y.; Ignea, C.; Kampranis, S. C. Transforming yeast peroxisomes into microfactories for the efficient production of high-value isoprenoids. *Proc. Natl. Acad. Sci. U.S.A.* **2020**, *117*, 31789–31799.
- (28) Gao, J.; Zhou, Y. J. Repurposing Peroxisomes for Microbial Synthesis for Biomolecules. *Methods in Enzymology*; Elsevier Inc., 2019; Vol. 617, pp 83–111.
- (29) Waterham, H. R.; Russell, K. A.; Vries, Y.; Cregg, J. M. Peroxisomal targeting, import, and assembly of alcohol oxidase in *Pichia pastoris*. *J. Cell Biol.* **1997**, *139*, 1419–1431.
- (30) Zhou, Y. J.; Buijs, N. A.; Zhu, Z.; Gomez, D. O.; Boonsombuti, A.; Siewers, V.; Nielsen, J. Harnessing yeast peroxisomes for biosynthesis of fatty-acid-derived biofuels and chemicals with relieved side-pathway competition. *J. Am. Chem. Soc.* **2016**, *138*, 15368–15377.
- (31) Shimazaki, S.; Yamada, R.; Yamamoto, Y.; Matsumoto, T.; Ogino, H. Building a machine-learning model to predict optimal mevalonate pathway gene expression levels for efficient production of a carotenoid in yeast. *Biotechnol. J.* **2023**, *19*, No. e2300285, DOI: 10.1002/biot.202300285.
- (32) Lu, S.; Zhou, C.; Guo, X.; Du, Z.; Cheng, Y.; Wang, Z.; He, X. Enhancing fluxes through the mevalonate pathway in *Saccharomyces*

*cerevisiae* by engineering the HMGR and  $\beta$ -alanine metabolism. *Microb. Biotechnol.* **2022**, *15*, 2292–2306.

(33) Guo, F.; Dai, Z.; Peng, W.; Zhang, S.; Zhou, J.; Ma, J.; Dong, W.; Xin, F.; Zhang, W.; Jiang, M. Metabolic engineering of *Pichia pastoris* for malic acid production from methanol. *Biotechnol. Bioeng.* **2021**, *118*, 357–371.

(34) Sarwar, A.; Lee, E. Y. Methanol-based biomanufacturing of fuels and chemicals using native and synthetic methylotrophs. *Synth. Syst. Biotechnol.* **2023**, *8*, 396–415.

(35) Cai, P.; Wu, X.; Deng, J.; Gao, L.; Shen, Y.; Yao, L.; Zhou, Y. J. Methanol biotransformation toward high-level production of fatty acid derivatives by engineering the industrial yeast *Pichia pastoris*. *Proc. Natl. Acad. Sci. U.S.A.* **2022**, *119*, No. e2201711119.

(36) Grewal, P. S.; Samson, J. A.; Baker, J. J.; Choi, B.; Dueber, J. E. Peroxisome compartmentalization of a toxic enzyme improves alkaloid production. *Nat. Chem. Biol.* **2021**, *17*, 96–103.

(37) Liu, G. S.; Li, T.; Zhou, W.; Jiang, M.; Tao, X. Y.; Liu, M.; Zhao, M.; Ren, Y. H.; Gao, B.; Wang, F. Q.; Wei, D. Z. The yeast peroxisome: A dynamic storage depot and subcellular factory for squalene overproduction. *Metab. Eng.* **2020**, *57*, 151–161.

(38) DeLoache, W. C.; Russ, Z. N.; Dueber, J. E. Towards repurposing the yeast peroxisome for compartmentalizing heterologous metabolic pathways. *Nat. Commun.* **2016**, *7*, No. 11152.

(39) Gao, N.; Gao, J.; Yu, W.; Kong, S.; Zhou, Y. J. Spatial-temporal regulation of fatty alcohol biosynthesis in yeast. *Biotechnol. Biofuels* **2022**, *15*, No. 141, DOI: 10.1186/s13068-022-02242-7.

(40) Zhai, X.; Gao, J.; Li, Y.; Grininger, M.; Zhou, Y. J. Peroxisomal metabolic coupling improves fatty alcohol production from sole methanol in yeast. *Proc. Natl. Acad. Sci. U.S.A.* **2023**, *120*, No. e2220816120.

(41) Rußmayer, H.; Buchetics, M.; Gruber, C.; Valli, M.; Grillitsch, K.; Modarres, G.; Guerrasio, R.; Klavins, K.; Neubauer, S.; Drexler, H.; Steiger, M.; Troyer, C.; Al Chalabi, A.; Krebiehl, G.; Sonntag, D.; Zellnig, G.; Daum, G.; Graf, A. B.; Altmann, F.; Koellensperger, G.; Hann, S.; Sauer, M.; Mattanovich, D.; Gasser, B. Systems-level organization of yeast methylotrophic lifestyle. *BMC Biol.* **2015**, *13*, No. 80, DOI: 10.1186/s12915-015-0186-5.

(42) Redding-Johanson, A. M.; Batth, T. S.; Chan, R.; Krupa, R.; Szmidt, H. L.; Adams, P. D.; Keasling, J. D.; Lee, T. S.; Mukhopadhyay, A.; Petzold, C. J. Targeted proteomics for metabolic pathway optimization: application to terpene production. *Metab. Eng.* **2011**, *13*, 194–203.

(43) Alonso-Gutierrez, J.; Kim, E. M.; Batth, T. S.; Cho, N.; Hu, Q. J.; Chan, L. J. G.; Petzold, C. J.; Hinson, N. J.; Adams, P. D.; Keasling, J. D.; Martin, H. G.; Lee, T. S. Principal component analysis of proteomics (PCAP) as a tool to direct metabolic engineering. *Metab. Eng.* **2015**, *28*, 123–133.

(44) Wei, S.; Wang, H.; Fan, M.; Cai, X.; Hu, J.; Zhang, R.; Song, B.; Li, J. Application of adaptive laboratory evolution to improve the tolerance of *Rhodotorula* strain to methanol in crude glycerol and development of an effective method for cell lysis. *Biotechnol. J.* **2024**, *19*, No. e2300483.

(45) Gao, J.; Li, Y.; Yu, W.; Zhou, Y. J. Rescuing yeast from cell death enables overproduction of fatty acids from sole methanol. *Nat. Metab.* **2022**, *4*, 932–943.

(46) Zhou, Y. J.; Gao, W.; Rong, Q.; Jin, G.; Chu, H.; Liu, W.; Yang, W.; Zhu, Z.; Li, G.; Zhu, G.; Huang, L.; Zhao, Z. K. Modular pathway engineering of diterpenoid synthases and the mevalonic acid pathway for miltiradiene production. *J. Am. Chem. Soc.* **2012**, *134*, 3234–3241.

(47) Fang, F.; Zhao, Q.; Chu, H. Y.; Liu, M. W.; Zhao, B. F.; Liang, Z.; Zhang, L. H.; Li, G. H.; Wang, L. M.; Qin, J.; Zhang, Y. K. Molecular dynamics simulation-assisted ionic liquid screening for deep coverage proteome analysis. *Mol. Cell. Proteomics* **2020**, *19*, 1724–1737.

(48) Bateman, A.; Martin, M. J.; Orchard, S.; Magrane, M.; Alpi, E.; Bely, B.; Bingley, M.; Britto, R.; Bursteinas, B.; Busiello, G.; Bye-A-Jee, H.; Da Silva, A.; De Giorgi, M.; Dogan, T.; Castro, L. G.; Garmiri, P.; Georghiou, G.; Gonzales, D.; Gonzales, L.; Hatton-Ellis, E.; Ignatchenko, A.; Ishtiaq, R.; Jokinen, P.; Joshi, V.; Jyothi, D.;

Lopez, R.; Luo, J.; Lussi, Y.; MacDougall, A.; Madeira, F.; Mahmoudy, M.; Menchi, M.; Nightingale, A.; Onwubiko, J.; Palka, B.; Pichler, K.; Pundir, S.; Qi, G. Y.; Raj, S.; Renaux, A.; Lopez, M. R.; Saidi, R.; Sawford, T.; Shypitsyna, A.; Speretta, E.; Turner, E.; Tyagi, N.; Vasudev, P.; Volynkin, V.; Wardell, T.; Warner, K.; Watkins, X.; Zaru, R.; Zellner, H.; Bridge, A.; Xenarios, I.; Poux, S.; Redaschi, N.; Aimo, L.; Argoud-Puy, G.; Auchincloss, A.; Axelsen, K.; Bansal, P.; Baratin, D.; Blatter, M. C.; Bolleman, J.; Boutet, E.; Breuza, L.; Casals-Casas, C.; de Castro, E.; Coudert, E.; Cuche, B.; Doche, M.; Dornevil, D.; Estreicher, A.; Famiglietti, L.; Feuermann, M.; Gasteiger, E.; Gehant, S.; Gerritsen, V.; Gos, A.; Gruaz, N.; Hinz, U.; Hulo, C.; Hykounou, N.; Jungo, F.; Keller, G.; Kerhornou, A.; Lara, V.; Lemercier, P.; Lieberherr, D.; Lombardot, T.; Martin, X.; Masson, P.; Morgat, A.; Neto, T. B.; Paesano, S.; Pedruzzi, I.; Pilbout, S.; Pozzato, M. UniProt: a worldwide hub of protein knowledge. *Nucleic Acids Res.* **2019**, *47*, D506–D515.

(49) Cox, J.; Hein, M. Y.; Lubner, C. A.; Paron, I.; Nagaraj, N.; Mann, M. Accurate proteome-wide label-free quantification by delayed normalization and maximal peptide ratio extraction, termed MaxLFQ. *Mol. Cell. Proteomics* **2014**, *13*, 2513–2526.

(50) Tyanova, S.; Temu, T.; Sinitcyn, P.; Carlson, A.; Hein, M. Y.; Geiger, T.; Mann, M.; Cox, J. The Perseus computational platform for comprehensive analysis of (prote)omics data. *Nat. Methods* **2016**, *13*, 731–740.

(51) Hou, R.; Gao, L.; Liu, J.; Liang, Z.; Zhou, Y. J.; Zhang, L.; Zhang, Y. Comparative proteomics analysis of *Pichia pastoris* cultivating in glucose and methanol. *Synth. Syst. Biotechnol.* **2022**, *7*, 862–868.